Journal of the European Ceramic Society 20 (2000) 1169–1178

A study of the Na_2O–CaO–P_2O_5–SiO_2 system with respect to the behaviour of phosphate bonded basic refractories at high temperature

M. Rivenet[a,*], O. Cousin[a], J.C. Boivin[a], F. Abraham[a], N. Ruchaud[b], P. Hubert[b]

[a]*Laboratoire de Cristallochimie et Physicochimie du Solide, ENSCL, BP108, 59652 Villeneuve d'Ascq cedex, France*
[b]*TRB, Unshaped and Pre-cast Refractories Manufacturer, Nesles, 62152 Neufchâtel-Hardelot, France*

Received 23 March 1999; received in revised form 13 September 1999; accepted 6 October 1999

Abstract

Investigating various phosphate bonded basic refractories by means of powder X-ray diffraction, energy dispersive spectroscopy and X-ray fluorescence analyses, reveals a relation between good mechanical properties at high temperature and the presence of a silicophosphate bond ($T > 1200°C$). The silicophosphate formation mechanism was studied using X-ray thermodiffractometry. From room temperature up to 500°C, a mixed calcium sodium phosphate gel is formed. It transforms around 500°C into a crystalline calcium sodium phosphate which is not stable at room temperature. Above 1200°C, the silicophosphate belongs to a $Na_{2-x}Ca_{5+x}(PO_4)_{4-x}(SiO_4)_x$ type solid solution with $x > 0$ identified by studying the Na_2O–CaO–P_2O_5–SiO_2 system. The $Na_{2-x}Ca_{5+x}(PO_4)_{4-x}(SiO_4)_x$ solid solution structure was shown to be a superstructure of the glaserite-type structure. Good mechanical properties of the refractory material are maintained as long as the silicophosphate glaserite-type unit cell superstructure is kept. That is achieved using starting raw materials with a high $\frac{CaO}{SiO_2}$ ratio and a high calcium content.

Keywords: Mechanical properties; Phase equilibria; Phosphate bonding; Refractories; X-ray methods

1. Introduction

During steel processing, the refractory linings which coat converters are subject to high mechanical stresses, thermal shock and slag attack. Moreover, additional localised effects such as erosion and thermomechanical strains lead to a fast wearing of three specific zones: the impact pad, the trunnions and the inferior slope levels (Fig. 1).[1] To offset the wearing of the converter linings, these zones are periodically repaired by gunning with a refractory powder. To be repaired, the converter is tilted over 90°. The nozzle of a gunning device is introduced through the aperture of the converter. The repairing powder, previously placed in the tank of the gunning equipment, is pushed out from the tank by air pressure, then mixed with water in the nozzle and sprayed on to the wall of the converter. Water addition is needed both for nozzle cooling and for setting of the repairing material. Although the setting is influenced by the gunning parameters and by the steel processing, it also depends on the material composition itself.[2,3] The material has to match the lining's characteristics: high dimensional stability, low porosity, high hot modulus of rupture, and limited interaction with slag. The powder/water mixture also needs to have specific additional properties like an optimum viscosity in order to prevent grain segregation during transportation and to ensure a good adhesion to the wall. In order to meet these various requirements, the gunning material is usually made from refractory raw materials (magnesia, dolomite, olivine, chromium oxide...), together with a binder (silicate, phosphate, chromate, sulphate) and other specific additives varying the rate of setting.[3] It has been previously shown that phosphate binders provide better high temperature mechanical properties than silicate or sulphate binders.[4–7] The phosphate type binder that is the most often used as the raw binder is more specifically a glassy sodium polyphosphate. The nature of the phosphate bond changes during the setting process. In the nozzle, when mixed with water, the phosphate

* Corresponding author.

0955-2219/00/$ - see front matter
PII: S0955-2219(99)00276-9

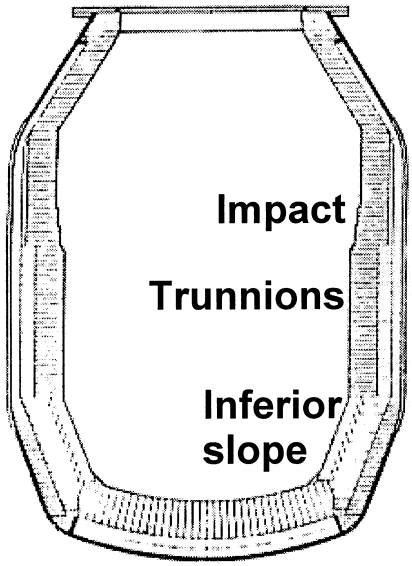

Fig. 1. The converter zones.

binder forms a gel. During the projection process, as the temperature of the gunning material increases from room temperature up to the temperature of the wall (about 1300°C), the bond nature evolves from a gel bond to a chemical bond. A ceramic bond finally takes place because of the temperature increase during steel processing.[6] The precise evolution depends on the gunning material composition and the temperature. Among the papers dealing with phosphate bonded basic materials, Di Bello et al.[4] described the high temperature bonding phase as an intergranular mixed calcium magnesium phosphate with composition $Ca_3Mg_3(PO_4)_4$. Lyon et al.[5] associated the bonding character to the phosphate glass $[Mg(PO_3)_2]_n$. Venable and Treffner[8] correlated the high mechanical properties of the material to the presence of rhenanite, α-$NaCaPO_4$, between 1000 and 1500°C, and to $Ca_3(PO_4)_2$ beyond 1500°C. Using SiO_2-bearing aggregates, Allaire and Rigaud[9] found evidence for a nagelschimidtite phase, $Ca_7(PO_4)_2(SiO_4)_2$,[10] instead of a rhenanite phase.

The present paper deals with the changes occurring within the phosphate bond between 1000 and 1700°C and the consequences for the mechanical behaviour of the gunning material at high temperature. In the first part, we describe the relation between the composition of the gunning material and the phases formed at high temperature. The second part shows the dependence of the mechanical properties on the heating temperature for three samples exhibiting different phosphate bond types. The correlation between the mechanical properties and the results of analyses performed by EDS, X-Ray diffraction, and X-ray fluorescence shows that the best results are obtained with a silicophosphate bonding phase. A contribution to the fundamental understanding of this phase is developed in the last section of the paper.

2. Experimental

All the investigated samples were made from calcined earth-magnesia (M), sodium polyphosphate, and calcium hydroxide (C). The presence of a small amount of calcium hydroxide increases the setting rate of the gunning material. It also improves adhesion and hot strength.[11] In some samples, part of the magnesia was replaced by olivine (Ø) or dolomite-clinker (D).

The grain distribution was optimised using the theoretical curve provided by Andreasen[12] with an n exponent equal to 0.35. The raw materials were thoroughly mixed in a Hobart type mixer and then added to 10 wt% of water. The resultant pastes were then cast in $40\times40\times160$ mm moulds and vibrated for 30 s. The samples were cured at room temperature for 30 min. After forming, the samples were removed from the moulds, then first heated at 1200°C for 1 h and, finally, at different selected higher temperatures for 5 h. The samples were cooled down in the furnace. To prevent structural spalling, the samples containing olivine were dried at 110°C for 24 h before being annealed.

In order to get a better understanding of the exact nature and the role of the phosphate and silicophosphate phases found to be present after heating, pure phases belonging to the Na_2O–CaO–P_2O_5–SiO_2 system were also synthesised. The phosphate syntheses were carried out using the following water dissolved precursors: calcium nitrate, sodium nitrate and 85% phosphoric acid. The silicophosphate phase was synthesised using sodium silicate instead of sodium nitrate. After evaporating the water, the nitrates were decomposed by heating the samples at 600°C. The resulting powder was then die-pressed and annealed at 1400°C during 6 h. After cooling, the phase purity was checked using X-ray diffraction. On occasion, an additional thermal treatment at 1400°C was required to obtain a pure phase.

Room temperature X-ray powder diffraction diagrams were recorded using a θ–2θ D5000 Siemens diffractometer equipped with a graphite monochromator in the back position. The phase identification was performed using the diffrac-at software of SOCABIM and the PDF data base of the JCPDS. All the diffraction diagrams were corrected for Cu-K_{α_2} radiation.

The thermodiffractograms were collected using a θ–θ D5000 Siemens diffractometer equipped with an Anton Paar high temperature device. The raw powder was laid on a fixed strip of platinum heated by the Joule effect. The Cu-K_α radiation was monochromated using a nickel filter.

X-ray microanalyses were performed by means of an energy dispersive spectrometer detector (EDAX PV

9900) connected to a Philips SEM-525M scanning microscope. A Si–Li detector supplied with an ultra-thin window made it possible to detect light elements. The analyses were performed on 2 cm^2 polished sections included in resin. The surfaces were covered with a thin carbon layer rather than a gold one to avoid interference with the phosphorus peaks. The results were corrected for matrix effects by means of the ZAF correction including atomic number, absorption and fluorescence corrections.

X-ray fluorescence analyses were carried out using a wavelength dispersive SRS300 Siemens spectrometer equipped with a rhodium anode (50 keV, 50 mA), proportional counters (flow and scintillation counters) and a sequential analyser. The samples were prepared using a lithium-based flux.

The cold modulus of rupture and the permanent linear change were measured respectively up to 1700 and to 1600°C on pre-heated samples. Hot modulus of rupture at 1500°C, refractoriness tests at 1600°C, refractoriness under load tests and thermal expansion measurements were carried out on the samples previously fired at 1200°C. NF and ASTM standard procedures were followed throughout.

The density of the powders was measured by means of a Micromeritics AccuPyc 1330 helium pycnometer with a 1 ml sample capacity.

3. Results and discussion

3.1. Raw materials characterisation

X-ray fluorescence analyses of the refractory raw materials are given in Table 1. The magnesia contains 1.4% (wt%) of CaO. The basic index, $\frac{CaO}{SiO_2}$, was shown to be equal to 0.5. According to the literature[13], a $\frac{CaO}{SiO_2}$ ratio lower than 1.86 leads, at high temperature, to the formation of mixtures of Mg_2SiO_4, $CaMgSiO_4$, $Ca_3Mg(SiO_4)_2$ and $MgAl_2O_4$ spinel at the MgO grain boundaries. The presence of such phases was confirmed by X-ray analysis of the samples previously heated at 1200, 1400 and 1600°C.

Olivine is a solid solution between Mg_2SiO_4 and Fe_2SiO_4. The used olivine contained 7.6% (wt%) of Fe_2O_3 which allows a high melting temperature to be maintained. Dolomite clinker is mainly constituted from CaO and MgO. The total amount of oxide impurities in the present raw material was equal to 4.7% within which ($Fe_2O_3 + Al_2O_3$) represents 2.3%. As in magnesia, impurities react to form phases which are segregated at the grain boundaries: X-ray diagrams show that the dolomite also contains minor quantities of Ca_3SiO_5 and $Ca(Fe,Al)_2O_5$.

The Graham salt $(NaPO_3)_n$ was used as the sodium polyphosphate. The average chain length, n, was calculated using the end group method described by Van Wazer[14] and the following equation suggested by Gustavsson and Larsson:[15] $n = \frac{2(\text{equivalents of strong acid groups})}{\text{equivalents of titrated weak acid groups}} = \frac{200}{a}$ where a is the volume of N/10 sodium hydroxide required to titrate 1.02 g of Graham's salt in the pH range 5.5–8.5. Calculation leads to an average of 15 units per chain in the selected polyphosphate which is suitable to obtain an efficient bond. In agreement with the literature, the polyphosphate chains must contain from 6 up to 21 $NaPO_3$ units.[4,7,16,17] Shorter as well as longer chains yield a lower bonding efficiency.[4,5] In the case of long chains, their instability in water leads to a random cut and to the appearance of short chains.[4]

The calcium hydroxide was shown to contain some $Ca_{1.5}SiO_{3.5}.xH_2O$.

3.2. Gunning materials composition

X-ray fluorescence analyses of the samples are reported in Table 2. The three compositions, MC, MD$^-$C and MDC, are based on magnesia (>60%) leading to a high MgO content (68 < MgO < 84wt%).

In the MD$^-$C and MDC materials, dolomite (D) respectively replaces 16 and 32% of the magnesia which yields the higher CaO concentration (12.3 and 20.3%) observed in these samples.

In the MØC samples, MgO is mainly brought by olivine (Ø) which is introduced in the replacement of 53% of the magnesia. Olivine is responsible for the large amount of Fe_2O_3 and SiO_2 (respectively 4.7 and 25.5%) found in these samples.

Small amounts of sodium polyphosphate and calcium hydroxide (<5%) were added to the refractory raw materials.

Table 1
Chemical compositions of the refactory raw materials

Refactory raw material	Composition (wt%)				
	Al_2O_3	SiO_2	Fe_2O_3	CaO	MgO
Magnesia	1.8	3.0	1.0	1.4	92.7
Olivine	0.2	42.0	7.6	0.1	49
Dolomite	1.2	2.4	1.1	56.4	38.3

Table 2
X-ray fluorescence analysis of the gunning materials

Gunning material	Main oxide contents (wt%)				
	SiO_2	Fe_2O_3	CaO	MgO	P_2O_5
MC	3.4	1.3	4.4	83.2	3.9
MD$^-$C	3.1	1.3	12.3	75.7	4.0
MDC	2.9	1.2	20.3	68.4	4.0
MØC	25.5	4.7	3.8	60.3	3.9

3.3. Phase composition of heated samples

X-ray diffraction patterns of all the samples confirm the presence of a large amount of MgO. However, the nature and quantity of other phases vary depending upon the overall composition and the heating temperature (Table 3).

MC samples exhibit minor quantities of forsterite, Mg_2SiO_4, and of a $Na_3Ca_6(PO_4)_5$[18] type phosphate from 1200 up to 1400°C. At higher temperature, the mixed sodium calcium phosphate tends to disappear and new phases such as $Ca_9MgNa(PO_4)_7$ or $NaCaPO_4$ can be found.

In the MD⁻C and MDC samples, the dolomite is responsible for the presence of calcium oxide, CaO, and hydroxide, $Ca(OH)_2$. The starting polyphosphate, $(NaPO_3)_n$, contributed to the formation of a mixed calcium sodium silicophosphate. The silicophosphate was identified using the powder data file of the definite compound, $Na_2Ca_4(PO_4)_2SiO_4$,[19] reported in the JCPDS. In those samples, the nature of the phases remains unchanged whatever the heating temperature in the investigated range. However, as the temperature is increased, the intensity of the silicophosphate X-ray reflections increased at the expense of that of CaO (Fig. 2). There is no free CaO left in the MD⁻C sample heated at 1600°C although there is some left in MDC. These results show that the formation of the silicophosphate requires the presence of dolomite which brings a large amount of calcium. This point will be discussed later. At high temperature, the MØC samples are characterised by the presence of large amounts of MgO and forsterite, Mg_2SiO_4. A minor phase, only found at 1200°C, could not be identified by X-ray diffraction. It probably corresponds to a mixed calcium magnesium sodium phosphate later revealed by microanalysis (see below). This phase progressively disappears beyond 1200°C leading to the formation of a spinel phase.

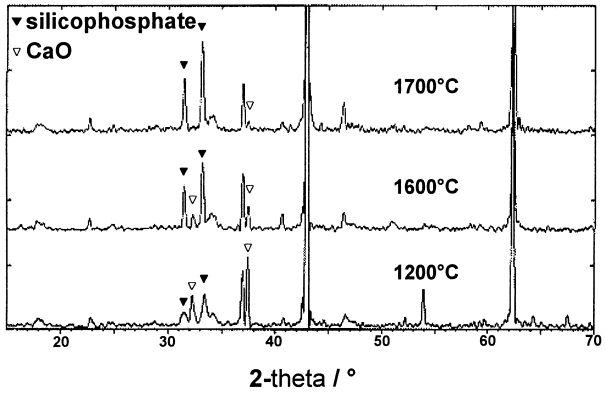

Fig. 2. X-ray diffraction diagrams of MDC samples versus the heating temperature.

3.4. Relation between mechanical properties and phase composition

The mechanical properties of the MC, MDC and MØC samples were studied versus the heating temperature. From Fig. 3, it can be seen that the MDC samples exhibit the highest cold modulus of rupture (CMOR) within the 1200–1700°C temperature range. Moreover, the increasing resistance of MDC samples from 1200 up to 1700°C is clearly associated with the increasing proportion of silicophosphate within the same range of temperatures (Fig. 2).

Although the presence of such a phase has already been mentioned in the literature, the conclusions about its influence on the mechanical properties have been contradictory. Davies and Carini,[20] Eguchi et al.,[21] Siegel and Waidacher[22] showed that the presence of silicophosphate leads to an increase of the mechanical properties whereas Venable and Treffner[8] concluded that the occurrence of silicophosphate in the gunning materials was unfavourable.

Table 3
Phase changes in the gunning materials with respect to the temperature[a]

Crystalline phases	MDC			MD⁻C			MC			MØC		
	1200	1400	1700	1200	1400	1700	1200	1400	1700	1200	1400	1700
MgO	******	******	******	******	******	******	******	******	******	*****	*****	*****
CaO	***	**	*	**	*							
$Ca(OH)_2$	*	*	*	*	*							
α-$Na_2Ca_4(PO_4)_2SiO_4$	**	**/***	***	**	**/***	***						
Mg_2SiO_4				*			**	**	**	******	******	******
$NaCaPO_4$									*			
$Na_3Ca_6(PO_4)_5$							**	**				
$Ca_9MgNa(PO_4)_7$									**			
Spinel phase											*	*
Phosphate phase										*	*	

[a] The number of asterisks indicates the phase proportion visually estimated by means of the main diffraction peaks intensities.

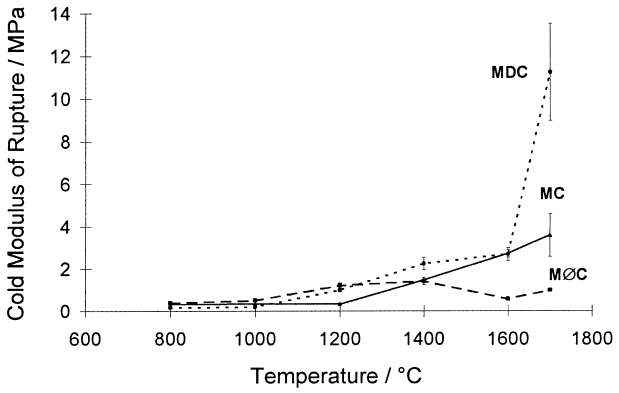

Fig. 3. Cold modulus of rupture of MC, MDC and MØC samples versus the heating temperature.

In order to clarify the role of the silicophosphate phases at high temperature, the microstructure of MDC samples annealed at 1400 and 1600°C was studied. The samples consist of MgO and dolomite grains. The MgO grains are slightly substituted by Na (~1.5% at.). The dolomite grains are hydrated and therefore covered by a criss-cross of $Ca(OH)_2$ crystals enabling EDS analysis in this domain. The presence of silicophosphate at the dolomite and MgO grains boundaries (Fig. 4) confirms the bonding character of this phase. Furthermore, EDS analyses show a non-homogeneous silicophosphate composition in the MDC sample heated at 1400°C (Table 4). Alongside dolomite grains, the mixed sodium calcium silicophosphate is slightly substituted by Al and Fe, whereas, at MgO grains boundaries, the silicophosphate phase is exclusively substituted by Mg. Although the silicophosphate (Si + P) content remains relatively the same (~35%), the silicon content is higher near dolomite than near MgO grains. At 1600°C, the silicophosphate composition becomes homogeneous. It is shown that sodium has volatilized out of the silicophosphate. The volatilized sodium (13%) is substituted by an equivalent amount of calcium of which the percentage rises from 43–49 to 61% (Table 4). The volatilization of sodium between 1400 and 1600°C, was confirmed by means of X-ray fluorescence analyses of the MDC samples (Fig. 5a).

According to the above results, the high temperature bond in MDC materials results from the reaction of the raw binder $(NaPO_3)_n$, with the intergranular silicate phases belonging to the basic raw materials. From 1200 up to 1400°C, this reaction leads to a mixed sodium calcium silicophosphate solid of $Na_{1-x}Ca_{1+x}(PO_4)_{1-x}(SiO_4)_x$[19] type. At higher temperature, the Ca^{2+} for Na^+ substitution shifts the bonding phase composition towards a calcium silicophosphate solid solution, $Ca_{2-x/2}(PO_4)_x(SiO_4)_{1-x}$. These changes do not affect significantly the X-ray diffraction pattern (Fig. 2). This behaviour suggests that the bonding phase belongs to the same structure type from 1200 up to 1700°C. The substitution $2Na^+ \leftrightarrow Ca^{2+} + \square$ might preserve the silicophosphate structure when Na_2O starts to volatilize and avoids, in this way, the degradation of the bonding phase at high temperature. It explains that good mechanical properties of the gunning materials require a high CaO content[4,7,21] or the presence of calcium silicates at the grain boundaries of the refractory materials.[23] The silicophosphate formation will be discussed in the

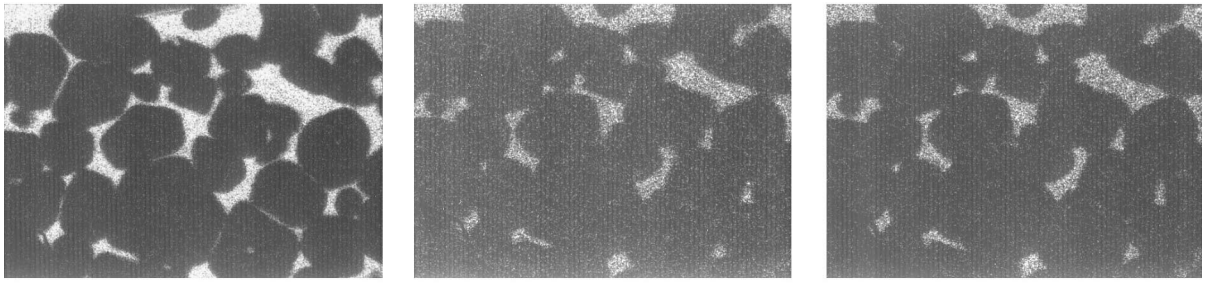

Fig. 4. X-images of Ca (a), Si (b) and P (c) elements along the MgO grains of a MDC sample fired at 1600°C.

Table 4
Microanalysis of the silicophosphate bonding phase in MDC samples pre-heated at 1400 and 1600°C

Temperature (°C)	Average atomic percentages of elements						
	Na	Al	Si	P	Ca	Fe	Mg
1400 (dolomite grains boundaries)	12.9	6.9	21.7	14.0	42.9	1.2	–
1400 (MgO grains boundaries)	12.7	–	15.6	18.7	49.5	–	2.6
1600	–	4.8	14.2	17.0	61.4	–	1.4

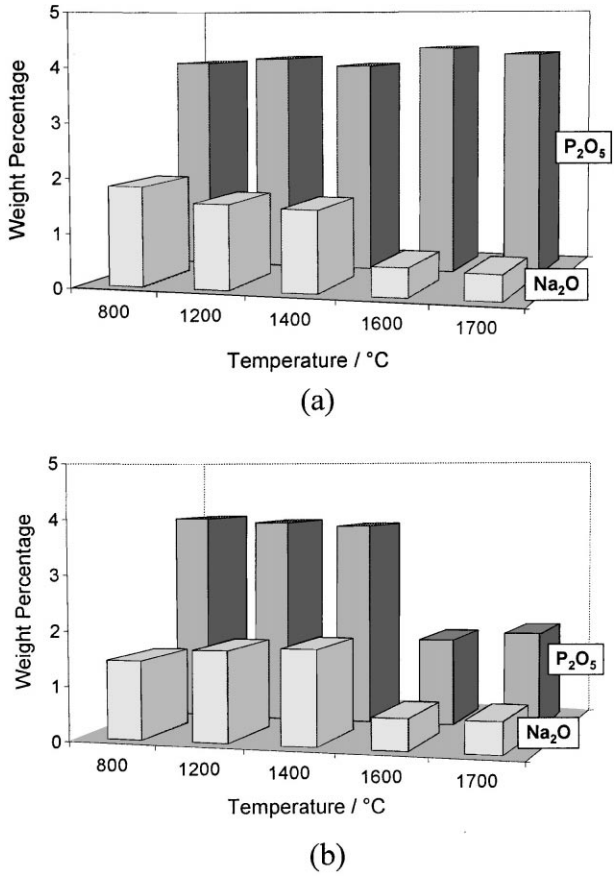

Fig. 5. Na_2O and P_2O_5 contents in MDC (a) and MØC (b) materials versus the heating temperature.

following section regarding the study of the Na_2O–CaO–P_2O_5–SiO_2 system.

In the MC samples, the total amount of CaO is too low to compensate for the Na_2O volatilization after heating at 1400°C. As a consequence, the phosphate $Na_3Ca_6(PO_4)_5$ decomposes into a different phosphate. This leads, at high temperature, to a lower strength than in the MDC samples.

X-ray microanalyses shows that a MØC sample heated at 1600°C contains a non-continuous intergranular phase identified as a mixed calcium magnesium sodium phosphate. The phosphorus content remains close to 39–40% (at. %). According to the literature,[8] magnesium substitution in a sodium calcium phosphate lowers the refractoriness. X-ray fluorescence analyses (Fig. 5b) confirmed that Na_2O and P_2O_5 volatilize out of MØC between 1400 and 1600°C. The decreasing resistance of MØC materials at high temperature is therefore associated with the volatilization of the bonding phase.

The better behaviour of MDC materials was confirmed by the hot modulus of rupture (HMOR) measurements which showed that the MC and MØC samples broke during the test whilst the MDC materials exhibited a HMOR equal to 0.3 MPa at 1500°C.

In order to prevent crack formation and propagation, the dimensional stability has to be high during the successive thermal heating and cooling cycles. From the permanent linear change measurements (Fig. 6), it can be seen that the volume variation of the MDC samples lies in the range −1, +1% up to 1600°C. The volume of MØC roughly varies within the same range. However, the samples show a higher shrinkage, up to −2%, at 1600°C. Refractoriness tests (Table 5) and refractoriness under load tests (Table 6) show that the MC and MØC samples exhibit high deformations. The behaviour of these materials can be explained by a strong sintering involving the formation of melted phases. In contrast, the low deformation of the MDC samples indicates that the sintering mainly involves solid state diffusion until 1600°C. The thermal expansion measurements confirmed that melted phases appear at lower temperature in MC and MØC than in MDC samples (Fig. 7).

The low refractoriness of the MØC samples is related to their high SiO_2 and Fe_2O_3 contents leading to the formation of easy melting phases. In MC materials, it is due to the high amount of magnesia with a low $\frac{CaO}{SiO_2}$ ratio which yields low melting point phases at the grain boundaries. The replacement of part of the magnesia by dolomite clinker increases the refractoriness of the samples and provides a higher dimensional stability.

3.5. The Na_2O–CaO–P_2O_5–SiO_2 system

According to the reciprocal salt diagram reported by Protsyuk et al.[24] (Fig. 8), the phosphate, $Na_3Ca_6(PO_4)_5$, which was identified in the MC material, belongs to the system $NaCaPO_4$–$Ca_3(PO_4)_2$. Ando et al.[18] found that $Na_3Ca_6(PO_4)_5$ corresponds to the limit of a solid solution of α-$NaCaPO_4$ structure, stabilised at low temperature. However, they did not give the lattice parameters.

The mixed calcium sodium silicophosphate solid solution evidenced in the MDC material was studied by

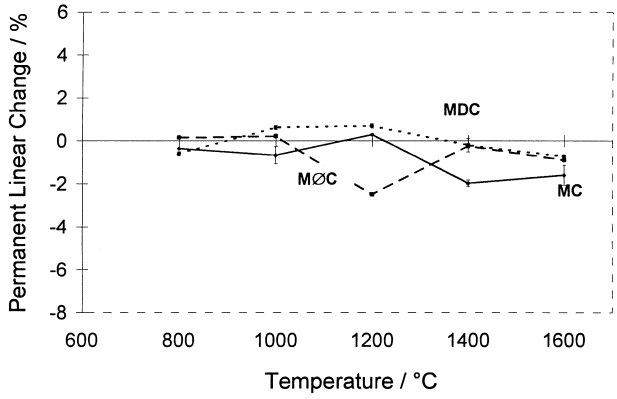

Fig. 6. Permanent linear change measurements of MDC, MØC and MC samples versus the heating temperature.

Table 5
Results of the refactoriness tests carried out by heating the samples at 1600°C for 5 h on 80 mm separated pillow-blocks

Gunning material	Deformation (%)[a]	
	Test 1	Test 2
MDC	3.75	1.25
MC	7.5	6.25
MØC	6.25	6.25

[a] The deformations, d, were calculated using $d(\%)=\frac{x}{l}\times 100$ where x and l are, respectively, the samples vertical sinking and length.

Table 6
Refractoriness under load measurements

Gunning material	Temperature (°C)[a]			
	T_0	$T_{0.5\%}$	$T_{2\%}$	$T_{5\%}$
MDC	1260	1410	1520	1575
MC	1335	1375	1380	1385
MØC	1270	1450	Rupture at 1550°C	

[a] T_0, $T_{0.5\%}$, $T_{2\%}$ and $T_{5\%}$ indicate, respectively, the temperatures for 0, 0.5, 2 and 5% deformation.

Kapralik et al.[19] It is a definite compound which forms a complete solid solution with α-$NaCaPO_4$ and α-Ca_2SiO_4, both isotypes with glaserite: $NaK_3(SO_4)_2$. On the basis of a double substitution, Na^+ for Ca^{2+} and P^{5+} for Si^{4+}, Kapralik et al.[19] calculated the lattice parameters $a=5.3653(7)$ and $c=7.158(2)$Å for the compound $Na_2Ca_4(PO_4)_2SiO_4$.

The literature review shows, therefore, that both the phosphate and silicophosphate are isotypes of α-$NaCaPO_4$, i.e. glaserite. Moreover, as can be seen in Table 7, their X-ray diffraction diagrams are close to that of the compound $Ca_7(PO_4)_2(SiO_4)_2$,[10] itself a member of the solid solution series, $Ca_{2-x/2}(PO_4)_x(SiO_4)_{1-x}$, which was identified in the MDC samples heated above 1400°C.

In order to find a possible relation between the structure of these bonding phases, physico-chemical characterisation of the phosphate $Na_3Ca_6(PO_4)_5$ and of the silicophosphate $Na_2Ca_4(PO_4)_2SiO_4$ was carried out.

The X-ray diffraction pattern of the synthesised $Na_3Ca_6(PO_4)_5$ is well defined and corresponds to the reference diagram reported in the PDF data base of the JCPDS. An hexagonal lattice was first determined by using the Dicvol 91 program.[25,26] The lattice parameters were later refined to $a=10.642(1)$ and $c=21.620(2)$Å. They indicate a superlattice $2a$, $3c$ of glaserite. The Smith and Snyder figure of merit, F_{20},[27] equal to 36.6 (0.0131, 43), shows good agreement between experimental and calculated data.

The X-ray diagram of the silicophosphate $Na_2Ca_4(PO_4)_2SiO_4$ was completely indexed using an hexagonal lattice also found by means of the program Dicvol 91.

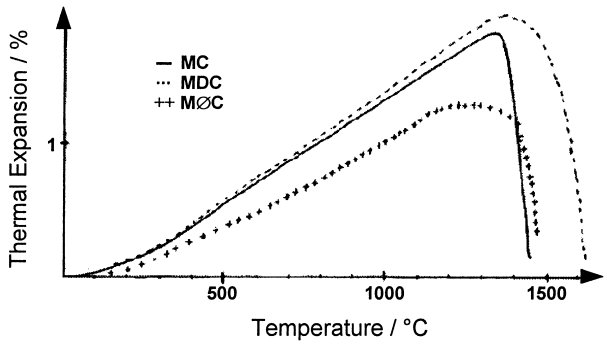

Fig. 7. Thermal expansion measurements of MDC, MØC and MC samples.

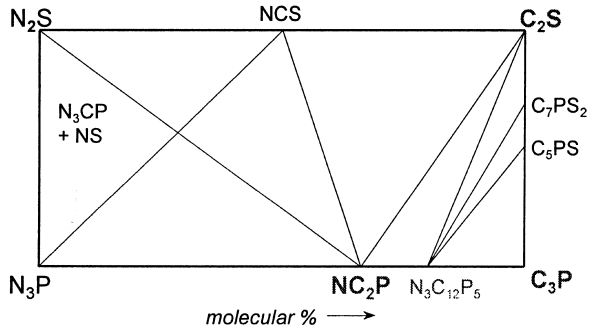

Fig. 8. The Ca_2SiO_4–$Ca_3(PO_4)_2$–Na_3PO_4–Na_4SiO_4 diagram as reported by Protsyuk et al.[24]

The refined parameters, $a=10.714(3)$ and $c=21.591(7)$Å, (with $F_{20}=27.3$ (0.0159, 54)) are close to those of the phosphate. They also constitute a superlattice of glaserite-type unit cell calculated by Kapralik et al.[19]

EDS analysis of the synthesised compounds showed that part of the sodium has volatilized during the thermal treatment. Moreover, the results pointed out that only part of the silicon has reacted to form the silicophosphate. The new formula of the phosphate, $Na_2Ca_5(PO_4)_4$, and silicophosphate, $NaCa_6(PO_4)_3(SiO_4)$, were shown to be somewhat different from the initial compositions (respectively, $Na_3Ca_6(PO_4)_5$ and $Na_2Ca_4(PO_4)_2SiO_4$).

The phosphate composition was confirmed by powder density measurement. The experimental density ($\rho=2.99$ g/cm^3) corresponds to 5 or 6 formula units per unit cell depending on the selected composition: $Na_3Ca_6(PO_4)_5$ or $Na_2Ca_5(PO_4)_4$, respectively. Owing to the multiplicity in an hexagonal group, the use of Z equal to 6 associated with a formula unit $Na_2Ca_5(PO_4)_4$ is the most realistic hypothesis ($\rho_{th}=2.94$ g/cm^3).

The phosphate $Na_2Ca_5(PO_4)_4$ had previously been evidenced by Ando et al.[28] in an other study of the $NaCaPO_4$–$Ca_3(PO_4)_2$ system. The authors suggested a hexagonal lattice parameter, a_0, twice the one refined in our study. However, indexation examination showed that the h indices in Ando's study were all even. Using $a_0/2$, as the parameter, the $Na_2Ca_5(PO_4)_4$ diagram was

Table 7
Powder data of $Na_3Ca_6(PO_4)_5$ (11-236), $Na_2Ca_4(PO_4)_2SiO_4$ (33-1229) and $Ca_7(PO_4)_2(SiO_4)_2$ (3-706)

Phosphate $Na_3Ca_6(PO_4)_5$		Silicorhenanite $Na_2Ca_4(PO_4)_2SiO_4$		Nagelschmidtite $Ca_7(PO_4)_2(SiO_4)_2$	
d (Å)	Int.	d (Å)	Int.	d (Å)	Int.
4.79	10	–	–	–	–
3.90	80	3.8971	19	3.93	40
3.60	20	3.5797	9	3.52	40
3.44	40	–	–	–	–
3.31	10	–	–	–	–
2.93	20	–	–	–	–
2.85	100	2.8353	80	2.86	100
2.67	100	2.6824	100	2.70	100
2.32	20	2.3231	4	2.33	20
2.20	40	2.2095	12	2.22	20
2.03	10	–	–	–	–
1.94	60	1.9486	25	1.96	100
1.80	20	1.7892	6	1.76	60
1.743	20	–	–	–	–
–	–	1.6695	3	1.67	40
–	–	1.5765	10	1.59	40
–	–	1.5502	6	1.56	40
1.490	20	1.4889	5	1.49	60
–	–	–	–	1.35	60

completely indexed using the same indices as that of the phosphate we synthesised. Two reflections, $d_{exp} = 2.720$ and $d_{exp} = 2.330$Å, indexed 008 and 208 by Ando can be advantageously indexed 215 and 109, respectively.

Although a large number of syntheses were undertaken varying the thermal treatment as well as the starting precursors, it was not possible to find final products with initial compositions $Na_3Ca_6(PO_4)_5$ and $Na_2Ca_4(PO_4)_2SiO_4$. According to the synthesis results, X-ray diffraction data, EDS analyses and density measurements, it is presumed that these compounds were respectively formulated by Ando et al.[28] and Kapralik et al.[19] without taking into account either the volatilization of Na_2O at high temperature or the low reactivity of silicon. It is assumed that the phosphate described as $Na_3Ca_6(PO_4)_5$ does not exist and is, actually, $Na_2Ca_5(PO_4)_4$, unfortunately unlisted in the PDF data base of the JCPDS.

On the basis of our results, and considering a double substitution mechanism, $Na^+ + P^{5+} \leftrightarrow Ca^{2+} + Si^{4+}$, a large domain of solid solution, $Na_{2-x}Ca_{5+x}(PO_4)_{4-x}(SiO_4)_x$ including the compositions $Na_2Ca_5(PO_4)_4$ ($x = 0$), $NaCa_6(PO_4)_3SiO_4$ ($x = 1$) and $Ca_7(PO_4)_2(SiO_4)_2$ ($x = 2$) could be formulated. According to Ando,[28] the $Na_2Ca_5(PO_4)_4$ structure is explained by formation of vacancies, when the $2Na^+ \leftrightarrow Ca^{2+} + \square$ substitution occurs in α-$NaCaPO_4$. The silicophosphate solid solution superstructure of the glaserite-type structure would, therefore, be due to the initial presence of vacancies in $Na_2Ca_5(PO_4)_4$. The new system $Ca_3(PO_4)_2$–Ca_2SiO_4–Na_4SiO_4–Na_3PO_4, redrawn with respect to our results, is shown in Fig. 9.

The large domain of stability of the silicophosphate solid solution helps to clarify the progressive formation of the silicophosphate bond evidenced by X-ray thermodiffractometry of the MDC material (Fig. 10). At room temperature, the high sequestrating power of $(NaPO_3)_n$ leads to a mixed sodium calcium phosphate gel occurring by means of an early reaction between Ca^{2+} ions and $(NaPO_3)_n$ mixed with water. This gel crystallises at around 500°C. As the temperature increases from about 800 to 900°C, the composition and lattice parameters of the crystalline calcium sodium phosphate precursor strongly evolve. The crystalline precursor is not stable at room temperature: it decomposes into $NaCaPO_4$ and $Ca_5(PO_4)_3OH$. From room temperature up to 1200°C, the solid solution precursor is, therefore, a complex calcium sodium phosphate. At higher temperature, the silicophosphate solid solution,

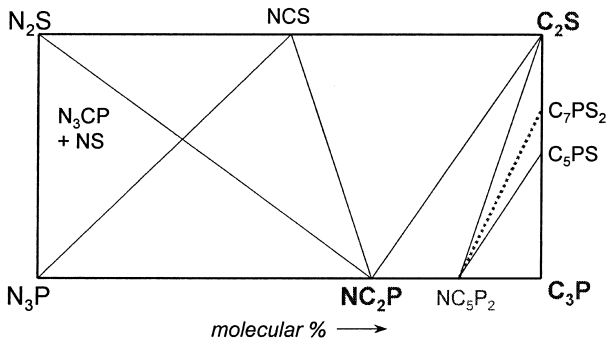

Fig. 9. The Ca_2SiO_4–$Ca_3(PO_4)_2$–Na_3PO_4–Na_4SiO_4 diagram redrawn on the basis of our results.

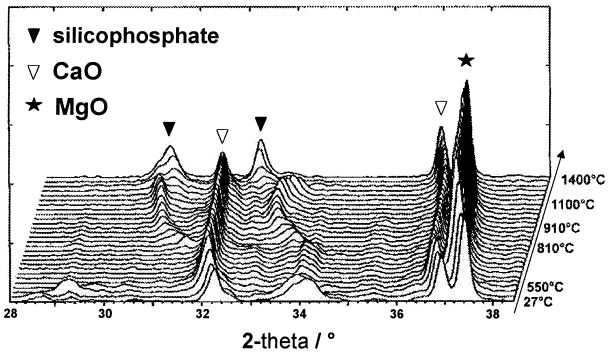

Fig. 10. X-ray thermodiffractometry of MDC sample showing the silicophosphate formation versus the heating temperature.

$Na_{2-x}Ca_{5+x}(PO_4)_{4-x}(SiO_4)_x$, is formed by reaction between the complex calcium sodium phosphate and the calcium silicates belonging to the basic refractory materials. Owing to the various intergranular silicate phases belonging to the basic raw materials, the substitution occurring in the solid solution is not limited to the double substitution $Na^+ + P^{5+} \leftrightarrow Ca^{2+} + Si^{4+}$. This explains the various substitution by Al, Fe and Mg observed during EDS analyses of the silicophosphate. After Na_2O has volatilized ($x \rightarrow 2$), the silicophosphate solid solution tends to a calcium silicophosphate solid solution as evident at the grain boundaries of MDC samples pre-heated at 1600°C.

4. Summary

Using powder X-ray diffraction and EDS analyses correlated with high temperature mechanical properties measurements, the present work has explained the better performance of silicophosphate-bonded compared to phosphate-bonded basic refractories.

The silicophosphate formation with the rising of the heating temperature was shown to be a continuous three step process leading, first to a mixed sodium calcium phosphate, then to a mixed sodium calcium silicophosphate and finally to a calcium silicophosphate. The formation of these different phases required: a high $(NaPO_3)_n$ sequestrating power, the presence of calcium silicates in the basic raw materials and a high calcium content.

The Na_2O–CaO–P_2O_5–SiO_2 system investigations emphasised the behaviour of the silicophosphate bond in the high temperature range. The silicophosphate was shown to belong to a $Na_{2-x}Ca_{5+x}(PO_4)_{4-x}(SiO_4)_x$ type solid solution which exhibits a glaserite-type supercell. As the temperature increases, Na_2O tends to volatilize, and owing to the high calcium content previously mentioned $2Na^+ \leftrightarrow Ca^{2+} + \square$ and $Na^+ + P^{5+} \leftrightarrow Ca^{2+} + Si^{4+}$ substitutions occur. The high temperature mechanical properties of the silicophosphate bonded materials was maintained as long as the silicophosphate solid solution structure was retained.

The $Na_{2-x}Ca_{5+x}(PO_4)_{4-x}(SiO_4)_x$ solid solution also showed a close relationship to the $Na_2Ca_5(PO_4)_4$, $NaCa_6(PO_4)_3SiO_4$ and $Ca_7(PO_4)_2(SiO_4)_2$ structures.

Acknowledgements

This work was supported by a grant from the "Région Nord-Pas de Calais" and the "Terres Réfractaires du Boulonnais" manufacturer. We are grateful to Professor J.B. Vogt from the "Laboratoire de Mátallurgie" of the University of Science and Technology of Lille for allowing us to access to the scanning microscope and EDS system and for fruitful discussions.

References

1. Motte, J. P., Beurotte, M., Provost, G., Foroglou, Z. and Antonopoulos, V., Optimisation des performances des revêtements de convertisseurs d'aciérie de Dunkerque. *Rev. Métall., May* 1988, 381–390.
2. Yount, J. G., Hot gunning materials for basic oxygen furnace maintenance. *Am. Ceram. Soc. Bull.*, 1968, **47**(3), 259–263.
3. Berthet, A. and Guenard, C., Contrôle des principaux paramètres de la réparation par projection des fours d'aciérie. *Rev. Métall.*, Jan. 1981, 1–13.
4. Di Bello, P. M. and Pradel, A. M., Performance of phosphate bonded refractory magnesias. *Interceram.*, 1968, **17** (3), 232–236; also, *J. Can. Ceram. Soc.*, 1968, **37**, 13–16.
5. Lyon, J. E., Fox, T. U. and Lyons, J. W., Phosphate bonding of magnesia refractories. *Ceram. Bull.*, 1966, **45**(12), 1078–1081.
6. Johnson, B., Recent developments in basic gunning refractories. *Proc. Electri. Furn. Conf.*, 1967, 87–88.
7. Limes, R. W., Bonds for gunning materials. *J. Metals*, 1965, **17**(5), 663–666.
8. Venable, C. L. and Treffner, W. S., X-ray study on phosphate bonding in basic refractories. *Ceram. Bull.*, 1970, **49**(7), 660–663.
9. Allaire, C., Rigaud, M. and Dallaire, S., Basic phosphate-bonded castables from dolomitic magnesite clinkers. *J. Am. Ceram. Soc.*, 1989, **72**(9), 1698–1703.
10. Bredig, M. A., Isomorphism and allotropy in compounds of type A_2XO_4. *J. Phys. Chem.*, 1942, **46**, 747–764.
11. Kurosaki Refractories Co., Ltd., View of development for gunning refractories. Technical Document, October 1979.
12. Andreasen, A. H. M. and Andersen, J., Über die beziehung zwischen kornabstufung und zwischenraum in produkten aus losen körnem (mit einigen experimenten). *Kolloid-Z*, 1930, **50**, 217–228.
13. Aliprandi, G., *Matériaux Réfractaires et Céramiques Techniques, Eléments de Céramurgie et de Technologie*. Septima, Paris, 1979 pp. 342–46.
14. Van Wazer, J. R., Structure and properties of the condensed phosphates. III. Solubility fractionation and other solubility studies. *J. Am. Chem. Soc.*, 1950, **72**, 647–655.
15. Gustavsson, K. H. and Larsson, A., The interaction of polymetaphosphates with hide protein. *Acta. Chem. Scand.*, 1951, **5**, 1221–1243.
16. Fuchs, R. J., Sodium phosphate glasses. United States Patent 3127238, 31 March 1964.
17. Bowman, J., Refractory bonding composition. United States Patent 3357843, 12 December 1967.

18. Ando, J., Phase diagrams of $Ca_3(PO_4)_2$–$Mg_3(PO_4)_2$ and $Ca_3(PO_4)_2$–$NaCaPO_4$ systems. *Bull. Soc. Japan*, 1958, **31**, 201–205.
19. Kapralik, I. and Hanic, F., Polymorphism and solid solutions in the system $2CaO.SiO_2$–$2CaO.Na_2O.P_2O_5$. *Trans. Brit. Ceram. Soc.*, 1977, **76**, 126–132.
20. Davies, B. and Carini, G. F., Magnesite refractories. United States Patent 3390002, 25 June 1968.
21. Eguchi, T., Ichiyama, H., Yoshimura, T., Kuroda, K. and Koga, M., Properties of CaO rich gunning material for converter. *Taïkabutsu overseas*, 1991, **11**(2), 44–46.
22. Siegel, W. M. and Waidacher, M., In *Proceedings of the International Symposium on Advances in Refractories for the Metallurgical Industries* II, ed. M. Rigaud and C. Allaire. Montréal, 1996, pp. 111–123.
23. Limes, R. W. and Russel, O., Basic refractory compositions. United States Patent 3304187, 14 February 1967.
24. Protsyuk, A. P., Pirogov, V. I., Galina, V. N., Tentler, L. G. and Azhikina, Yu. V., Subsolidus structure of the partial system Na_2O–CaO–$Ca_3(PO_4)_2$–Na_3PO_4–Na_2SiO_3–$CaSiO_3$. *Neorg. Mater.*, 1981, **17**(9), 1721–1722.
25. Louer, D. and Louer, M., Méthode d'essais et erreurs pour l'indexation automatique des diagrammes de poudre. *J. Appl. Crystallogr.*, 1972, **5**, 271–275.
26. Boultif, A. and Louer, D., Indexing of powder diffraction patterns for low symmetry lattices by the successive dichotomy method. *J. Appl. Crystallogr.*, 1991, **24**, 987–993.
27. Smith, G. S. and Snyder, R. L., A criterion for rating powder diffraction patterns and evaluating the reliability of powder-pattern indexing. *J. Appl. Crystallogr.*, 1979, **12**, 60–65.
28. Ando, J. and Matsuno, S., $Ca_3(PO_4)_2$–$CaNaPO_4$ system. *Bull. Soc. Japan*, 1968, **41**, 342–347.